



저작자표시-비영리-변경금지 2.0 대한민국

이용자는 아래의 조건을 따르는 경우에 한하여 자유롭게

- 이 저작물을 복제, 배포, 전송, 전시, 공연 및 방송할 수 있습니다.

다음과 같은 조건을 따라야 합니다:



저작자표시. 귀하는 원저작자를 표시하여야 합니다.



비영리. 귀하는 이 저작물을 영리 목적으로 이용할 수 없습니다.



변경금지. 귀하는 이 저작물을 개작, 변형 또는 가공할 수 없습니다.

- 귀하는, 이 저작물의 재이용이나 배포의 경우, 이 저작물에 적용된 이용허락조건을 명확하게 나타내어야 합니다.
- 저작권자로부터 별도의 허가를 받으면 이러한 조건들은 적용되지 않습니다.

저작권법에 따른 이용자의 권리는 위의 내용에 의하여 영향을 받지 않습니다.

이것은 [이용허락규약\(Legal Code\)](#)을 이해하기 쉽게 요약한 것입니다.

[Disclaimer](#)

공학석사학위논문

트래픽 알림을 활용한 폴링 기반
LoRaWAN 다운링크 통신 프로토콜

Polling-Based Downlink Communication Protocol
for LoRaWAN using Traffic Indication

2019년 2월

서울대학교 대학원
컴퓨터공학부

오 영 준

트래픽 알림을 활용한 폴링 기반
LoRaWAN 다운링크 통신 프로토콜

Polling-Based Downlink Communication Protocol
for LoRaWAN using Traffic Indication

지도교수 김 종 권
이 논문을 공학석사학위논문으로 제출함

2018년 10월

서울대학교 대학원
컴퓨터공학부
오 영 준

오영준의 석사학위논문을 인준함

2018년 12월

위 원 장 전 화 숙 (인)

부 위 원 장 김 종 권 (인)

위 원 권 태 경 (인)

ABSTRACT

Polling-Based Downlink Communication Protocol for LoRaWAN using Traffic Indication

Youngjune Oh

Dept. of Computer Science and Engineering

The Graduate School

Seoul National University

LPWAN (Low Power Wide Area Network) technologies such as LoRa and SigFox are emerging as a technology of choice for the Internet of Things (IoT) applications where tens of thousands of untethered devices are deployed over a wide area. In such operating environments, energy conservation is one of the most crucial concerns and network protocols adopt various power saving schemes to lengthen device lifetimes. For example, to avoid idle listening, LoRaWAN restricts downlink communications. However, the confined design philosophy impedes the deployment of IoT applications that require asynchronous downlink communications. In this thesis, we design and implement an energy efficient downlink communication

mechanism, named TRILO, for LoRaWAN. We aim to make TRILO be energy efficient while obeying an unavoidable trade-off that balances between latency and energy consumption. TRILO adopts a beacon mechanism that periodically alerts end-devices which have pending downlink frames. We implement the proposed protocol on top of commercially available LoRaWAN components and confirm that the protocol operates properly in real-world experiments. Experimental results show that TRILO successfully transmits downlink frames without losses while uplink traffic suffers from a slight increase in latency because uplink transmissions should halt during beacons and downlink transmissions. Computer simulation results also show that the proposed scheme is more energy efficient than the legacy LoRaWAN downlink protocol.

Keywords: Low Power Area Network, LoRa, LoRaWAN, Network Communication Protocol, Downlink Communication, Internet of Things, Traffic Indication

Student Number: 2017-26321

CONTENTS

ABSTRACT	i
CONTENTS	iii
LIST OF FIGURES	iv
LIST OF TABLES	vi
CHAPTER I: Introduction	1
CHAPTER II: Related Work	8
CHAPTER III: A Primer on LoRa and LoRaWAN	11
CHAPTER IV: Downlink Communications Scheme	17
4.1 Comparison of Two Polling Schemes	19
4.2 Proposed Downlink Communications Scheme	26
CHAPTER V: Implementation	28
CHAPTER VI: Evaluation	31
6.1 Experimental Results	32
6.2 Simulation Results	37
CHAPTER VII: Discussion	42
CHAPTER VIII: Conclusion	45
BIBLIOGRAPHY	47
초록	51

LIST OF FIGURES

Figure 3.1 LoRa and LoRaWAN specifications	11
Figure 3.2 Class A end-device initiated uplink and responding downlinks	14
Figure 3.3 Beacon based Class B downlink scheme	15
Figure 4.1 Beacon and poll message formats (a) Beacon (b) Poll	18
Figure 4.2 Example of polling mechanisms (a) Concurrent polling (b) Sequential polling	20
Figure 4.3 Performance of concurrent polling and sequential polling (a) Average wake-up time of both idle and busy devices (b) Average wake-up time of busy devices	24
Figure 4.4 Proposed downlink communication scheme	27
Figure 5.1 Devices used for implementation (a) End-device with SX1272MB2DAS attached to a NUCLEO-L073RZ board (b) Gateway with RAK831 attached to a Raspberry Pi 3	28
Figure 5.2 Block diagram of a network server that handles beacon and poll messages	29
Figure 6.1 Experiment environment. One gateway (yellow dot) and 15 end-devices (blue dots) are deployed in our office building	32

Figure 6.2 Duty cycles required for downlink operation including beacon, poll, and downlink data transmissions	34
Figure 6.3 Average latency of traffic.	
(a) Downlink latency	
(b) Uplink latency	35
Figure 6.4 Efficiency of TRILO and Class B downlink protocol	40
Figure 7.1 False positive ratio of 2-phase bloom filter of 96-bit array 1-phase filter with various size of 2-phase filter	43
Figure 7.2 Total wake-up time for polling and downlink operation ..	44

LIST OF TABLES

Table 3.1 Frequency bands and bandwidths allocated for LoRa	13
Table 4.1 Notations for analysis of poll mechanisms	20
Table 6.1 Packet delivery ratio of uplink traffic at various uplink and downlink offered loads	33
Table 6.2 Notations used for Class B downlink protocol and TRILO	38

Chapter I

Introduction

The Internet of Things (IoT) interconnects “all” things including sensors, actuators, gateways, and everyday products such as watches and various wearable devices. The IoT ecosystem includes heterogeneous applications with diversified performance and functional requirements. To support diversified IoT applications operating on a broad spectrum of devices, multiple heterogeneous technologies should be harmoniously applied. The exigency of applying plural enabling techniques is particularly apropos in the area of networking; a single network technique cannot satisfy contradictory networking requirements of diverse IoT applications. In addition to traditional wireless network technologies such as cellular and WiFi networks, a plethora of WPAN (Wireless Personal Area Network) schemes including ZigBee, Z-Wave, IETF 6LowPAN, and Bluetooth Low Energy (BLE) can easily find areas of applications in the IoT ecosystem. Equipped with low-cost and power conserving capabilities, these network technologies compensate functional or economical cracks engendered by cellular or WiFi networks. However, most WPAN technologies are designed for short range communications and consume abundant energy to support low latency asynchronous bidirectional communications.

Recent years have witnessed explosive attentions on Low-Power Wide Area Network (LPWAN) technology as a means to fill the gap that existing network technologies leave behind. LPWAN targets to provide low-rate, high-latency communication capabilities to large

numbers of IoT devices that are scattered over expanded areas such as campus, town, or city [1, 2]. Because it is difficult to manage widely scattered devices, LPWAN protocols are designed to sustain the lifetimes of devices more than ten years with a coin cell battery. To achieve both the long-range transmission and energy conservation goals, LPWAN adopts robust modulation and simple one-way communication protocols, respectively.

Among many LPWAN alternatives, this thesis deals with the LoRa [3] and LoRaWAN [4, 5] technologies. LPWAN technologies can be classified into two categories: one operating in licensed bands and another in unlicensed bands. The 3GPP [6 - 9] has standardized two open standard protocols called LTE-M and NB-IoT [10, 11] that utilize the cellular infrastructure. Recently, Lauridsen et al. [12] reported extensive experimental performance results which show that NB-IoT and LTE-M schemes have contradictive characteristics and each has an advantage over the other depending on application areas. LoRa [3], SigFox [13], RPMA [14], and Weightless [15] are examples of noncellular technologies that operate in unlicensed spectrums. In addition to the free use of wireless spectrum resources, LPWAN technologies provide the advantages of network ownership and autonomous operation of networks. However, most of the LPWANs are proprietary techniques and cannot leverage the widely deployed cellular infrastructure.

Employing robust and less efficient modulation and sacrificing transmission speed, LoRa achieves long-range transmissions over 10 km. In addition, LoRaWAN achieves an unprecedented energy conservation capability by restricting downlink communications. LoRaWAN Class A end-devices stay in the sleep state as a norm and wake up only when they need to transmit uplink traffic. While

LoRaWAN supports uplink transmissions like other protocols, downlink transmissions are allowed only as a response to uplink packets. As a result, LoRaWAN eliminates idle listening, a root cause of energy consumption in communications. These characteristics and limitations of LoRa and LoRaWAN indicate that they are optimized for applications that do not require high throughput or low latency data delivery.

In this thesis, we embark on the design of an energy conservative downlink communication protocol on top of the LoRaWAN protocol. Let us start with a brief introduction of the LoRaWAN protocol. LoRaWAN forms a star-of-stars topology consisting of end-devices, gateways, and servers. A server is connected to multiple gateways each of which again is connected to multiple end-devices. A gateway assumes a role similar to a WiFi Access Point (AP). A gateway is connected to multiple end-devices via the LoRa wireless technology. Note that a LoRaWAN does not support multihop wireless transmissions; all end-devices are directly connected to gateways. LoRa is particularly designed for massive IoTs over a wide area, and a single LoRaWAN network can support tens of thousands of end-devices each of which emits short packets infrequently.

LoRaWAN defines three classes of end-devices depending on the level of energy conservation and the demands for downlink transmissions. A Class A node abnegates the reception of asynchronous downlinks by staying mostly in a sleep mode turning off its radio. It only wakes up for uplink transmissions as such demands occur. Class C end-devices operate in an always-on mode which allows asynchronous downlinks as well as uplinks. Class C end-devices assume the continuous supply of power, or their lifetimes would be much shorter than those of Class A devices. Class B

end-devices also support downlinks in addition to uplink transmissions. Unlike uplink transmission that can be initiated at any time, downlinks should be synchronously scheduled according to the requests from end-devices. They use beacons to maintain time synchronization between a server and end-devices. Class B nodes wake up at scheduled intervals periodically even if there are no downlinks for them. We aim to devise a new downlink protocol which aims to be more energy efficient and flexible than the LoRaWAN's Class B downlink scheme.

The proposed downlink protocol, named TRILO, is based on the beacon mechanism. Like the IEEE 802.11 WLANs where an AP coordinates communications of multiple mobile stations, a gateway in a LoRaWAN can broadcast frames to all end-devices. Beacons are an efficient signalling mechanism because a broadcast beacon can alert multiple end-devices with a single message. In addition to beacons, a polling mechanism to announce the readiness to receive downlinks must be provided. A polling scheme should be designed carefully such that it fully exploits the physical characteristics of the underlying LoRa protocol. We consider two polling alternatives: concurrent polling and sequential polling. We choose sequential polling because a performance comparison indicates that sequential polling is more effective in power saving than concurrent polling (see Figure 4.2).

We implemented TRILO on commercially available LoRaWAN components. For a gateway, we used a RAK831 board which contains a SX1301 concentrator chip. The concentrator board is attached to a Raspberry Pi 3 board. An end-device is implemented on a NUCLEO-L073RZ board with an embedded LoRaWAN chip using 915Mhz antenna. The SX1272MB2DAS component is attached to a NUCLEO-L073RZ board with a modified LoRaMAC that includes our

proposed scheme. Note that a network server and end-devices are communicating entities in the LoRaWAN architecture; gateways assume a passive role relaying frames between end-devices and a server.

We confirmed that the devised downlink protocol works correctly via real-world experiments. Extensive experiments were also conducted to collect important performance measures such as PDR (Packet Delivery Ratio), latency, and power consumption. An experimental network, which consists of one gateway and 15 end-devices, is deployed to our office building. Experimental results show that TRILO operates correctly. All end-devices receive beacons and downlink frames successfully. The PDR of downlinks is almost 100% in most experiment setups. Under an assumption that downlink traffic to each end-device is not heavy, the extra wake-up times required for maintaining and supporting downlink frame transmissions are minimal.

We also compare the performance of TRILO with that of Class B downlink protocol via computer simulations. Power consumption is an important performance metric in LoRaWAN. We measure the efficiency of downlink protocols which is the ratio of the actual data transmission time to the duty cycle. Simulation results show that the proposed protocol performs significantly better than the Class B scheme. The proposed scheme shows 3.7 times to about 14.6 times better efficiency than the Class B downlink protocol.

The contributions of this thesis are as follows.

- We propose a new energy efficient downlink protocol, called TRILO, for LoRaWAN. TRILO is customized to the physical and network properties of LoRa and LoRaWAN. In particular, we aim to

devise a protocol that is more energy efficient than synchronous downlink mechanism developed for LoRaWAN's Class B.

- We devise two polling mechanisms called concurrent polling and sequential polling. Concurrent polling best exploits the LoRa's capability that supports simultaneous receptions of multiple packets. However, the analysis indicates that sequential polling is more energy efficient than concurrent polling, and we adopt sequential polling.
- TRILO is implemented on commercially available LoRaWAN components. Modified LoRaWAN components operate properly in real-world experiments.
- We conduct experiments with modified LoRaWAN devices. Our performance study shows that PDR is almost 100% for both uplink and downlink traffic and the extra wake-up times to maintain and support beacons and downlink packets are minimal.
- We conduct computer simulations to compare the performances of TRILO and the LoRaWAN's Class B downlink protocol. Our performance study shows that the proposed scheme, which minimizes unnecessary receive window allocations, is significantly more energy efficient than the legacy LoRaWAN.

The rest of the thesis is organized as follows. We begin with the related work highlighting several low-power MAC mechanisms. We then give a brief primer on LoRa and LoRaWAN focusing on the features of LoRa and LoRaWAN that are closely related to the design of downlink protocols. Next, we describe the proposed beacon based downlink protocol. Two polling methods, concurrent polling and sequential polling, are explained. We compare the wake-up times of the two polling methods and show that sequential polling is more energy efficient than concurrent polling. Then, the implementation

details of TRILO and performance results obtained from real-world experiments are described. We also illustrate the performance comparison of TRILO and the LoRaWAN's downlink protocol. In addition, we discuss the idea for foreseeable overhead of our protocol. Lastly, conclusion summarizes the thesis and discusses several future research problems.

Chapter II

Related Work

Energy is one of the precious resources that should be managed carefully in battery powered mobile devices. Many researchers have studied energy conservation schemes in various scenarios. This section reviews several exemplary power saving schemes.

Basically, almost all energy conservation schemes try to minimize the duty cycle. The literature can be partitioned into two categories depending on the type of communications: one to one communications and one to many communications. Usually, one to one communication is between two devices of the equal capabilities. On the other hand, in most one to many networks, a central node enjoys unlimited power supply from a powerline while many others are battery powered mobile devices. For example, a WiFi network consists of one AP (Access Point) and many mobile stations. As most prior works, we focus on the energy conservation for battery powered devices.

Many clever low-power MAC mechanisms have been designed for WSNs (Wireless Sensor Networks) which implement multihop wireless networks over WiFi networks or the IEEE 802.15.4 standard protocols. Even though base network technologies support one to many communications, neighbour nodes in mesh networks assume peer to peer communications. The energy conservation mechanisms for WSNs can be classified by several criteria such as synchronicity and sender- or receiver-initiated. The two most widely deployed protocols,

ContikiMAC [16, 17] and TinyOS LPL [17, 18], are asynchronous sender-initiated protocols and are implemented on two de facto standard operating systems, Contiki [16] and TinyOS [18], respectively. In sender-initiated protocols, a sender transmits a packet repeatedly for a time longer than a predetermined duty cycle interval. A receiver operates in the duty cycling mode; it wakes up at every duty cycle interval and listens for a possible transmission from the sender.

Bluetooth Low Energy (BLE) [19] is another network technology that requires one to one energy conserving MAC. BLE aims for the lifetime from several months to years with a coin cell battery [19]. The BLE neighbour (device) discovery mechanism is an asymmetric scheme where each device plays the role of either an advertiser or a scanner. To bind with another BLE device, an advertiser transmits advertising packets periodically at every scheduled advertising event. A scanner also turns its radio on repeatedly at every scanning events. Applying the Chinese Remainder Theorem, Kandhalu, Xhafa, and Hosur [20] devised a BLE neighbour discovery mechanism that guarantees eventual rendezvous of advertisers and scanners. To avoid the ill-fated case that both advertiser and scanner choose the same prime number, each device selects two prime numbers and wakes up at every integer multiples of the primes.

Several researchers have proposed new neighbour discovery schemes that reduce discovery latency, power consumption, and reliability of the BLE device discovery mechanism. Unlike the legacy BLE devices whose roles are fixed to either advertiser or scanner at the production time, [21] assumed that devices could change their roles dynamically. They devised a new neighbour discovery protocol customized for such environments. Contrary to the prior methods that use time slots, BLEnd [22] demises the slot structure and reduces the discovery delay.

Nihao [23] improves the latency and reduces energy consumption by increasing advertisements and decreasing scanning times.

One notable energy conservation protocol for one to many communications is the IEEE 802.11 PSM (Power Saving Mode). An Access Point (AP) periodically broadcasts beacons to notify mobile stations that have pending downstream frames. Inspecting a beacon frame, idle stations without buffered downlinks turn their radio off immediately until the next beacon interval. Backlogged stations request for downstream packet transmissions by sending poll messages to the AP. Upon the delivery of downlink frames, backlogged stations also fall back to the sleep state until the next beacon.

Chapter III

A Primer on LoRa and LoRaWAN

This section contains a brief overview of LoRa and LoRaWAN technologies. Specifically, technical properties that influence or limit the design space of LoRaWAN based downlink protocol will be addressed.

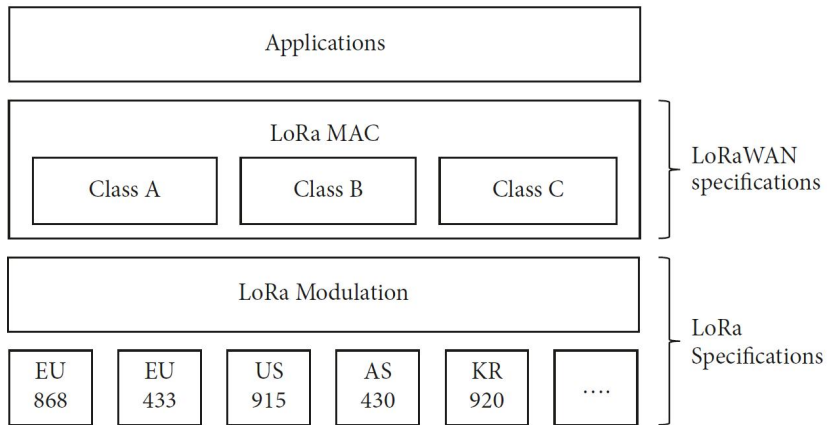


Figure 3.1: LoRa and LoRaWAN specifications.

Figure 3.1 shows the protocol stack of LoRa and LoRaWAN [4]. LoRa, developed and owned by Semtech [3], is a propriety technique that defines a physical layer customized for LPWA communications. LoRaWAN, which defines a MAC layer on top of LoRa, is an open standard developed by a nonprofit organization called LoRa alliance. LoRa operates on the 900 MHz ISM spectrum and adopts the CSS

(Chirp Spread Spectrum) modulation technique. CSS [24, 25], based on chirped-FM modulation, yields high processing gains and enables long transmissions at the expense of data rates. LoRa supports Adaptive Data Rate (ADR) which varies data rates adapting to transmission distances and channel conditions. When the SNRs are low, LoRa lowers the data rate to several hundred bits per second by using large SF (Spreading Factor) and robust CR (Coding Rate). When SF and bandwidth (BW) are selected, the data rate, R_{SF} , is determined as $SF/2^{SF} \times BW$. The lowest data rate of LoRa, determined at SF=12 and BW=125 KHz, is approximately 300 bits per second. The highest data rate is approximately 11 Kbps and is obtained at SF=7 and BW=250 KHz. High data rates can be achievable when channel conditions are good; SF=7 requires -120 dBm while SF=12 requires only -136 dBm.

Each country allocates different frequency bands and bandwidth for LoRa. Table 3.1 illustrates the frequency bands, bandwidth, and transmission powers defined by the regulatory bodies at several regions and countries. It is worthwhile to note that a device that locks on one SF can successfully receive a signal even though signals of different SF exist at the same time on the same subchannel. Moreover, gateways can simultaneously receive multiple transmissions if either subchannels or SFs are different. Currently, the SX1301 based gateway supports concurrent demodulations up to 8 signals.

Table 3.1: Frequency bands and bandwidths allocated for LoRa

Location	Europe	North America	Korea	China	Japan
Frequency band(MHz)	867-869	902-928	920-923	470-510/ 779-787	920-925
Channels	10	64+8+8	13	-	-
Uplink CH BW(KHz)	125/250	125/500	125	-	-
Downlink CH BW(KHz)	125	125	125	-	-
Tx power Up (dBm)	+14 dBm	+20 ~ +30 dBm	+10 ~ +14 dBm	-	-
Tx power Down (dBm)	+14 dBm	+27 dBm	+23 dBm	-	-

LoRa's CSS modulation enables packet receptions even when the signal power is much less than the absolute noise floor. The high reception sensitivity makes carrier sensing practically impossible. Lack of carrier sensing forces the original LoRa to use the Aloha MAC that suffers from excessive collisions. Even though some countries require LBT (Listen Before Talk), it is quite difficult to sense on-going LoRa signals without synchronizing with preambles. This thesis assumes that all devices use the Aloha MAC.

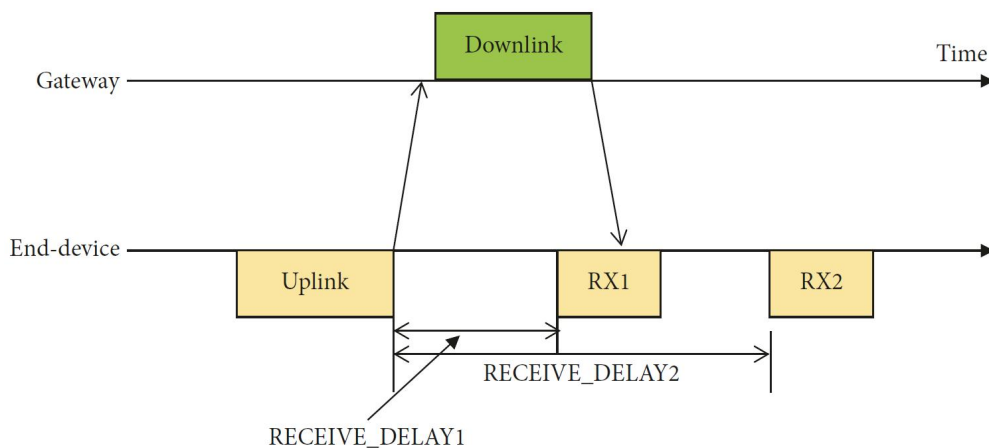


Figure 3.2: Class A end-device initiated uplink and responding downlinks.

The LoRaWAN end-devices are classified into three classes, Classes A, B, and C. A Class A device—bidirectional end-devices—can initiate uplink transmissions only. It can receive downlink frames, but only as a response to uplink frames that it has initiated. Figure 3.2 describes the timing of an initial uplink transmission and following downlink transmissions. The timing of downlink transmissions should be carefully coordinated; the server should schedule a downlink such that its transmission interval is coincident with predetermined receive windows. Class A end-nodes sacrifice asynchronous downlink transmissions but attain long lifetimes as a reward. It is expected that battery powered Class A end-devices enjoy ten to twenty years of lifetimes in reasonable use cases. Class A is suitable for sensor nodes that report sensing data periodically or when the readings satisfy predetermined criteria.

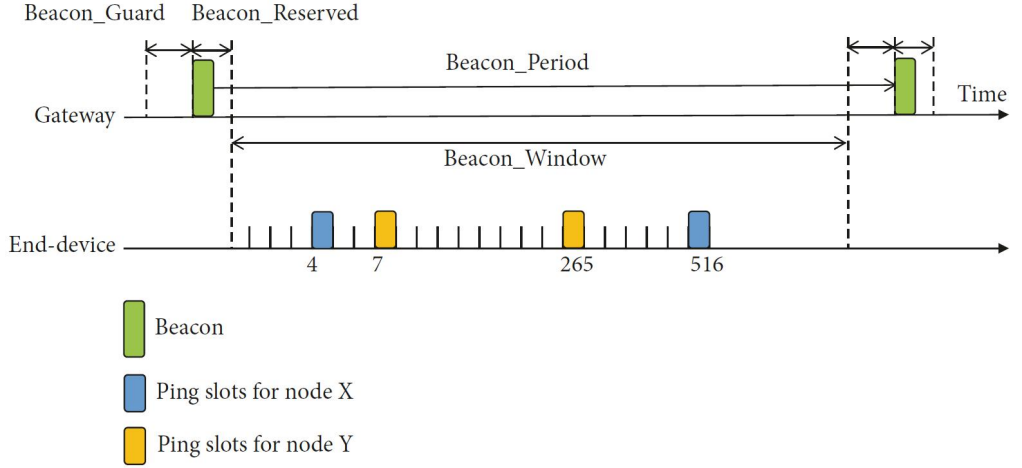


Figure 3.3: Beacon based Class B downlink scheme.

Unlike a Class A end-device, Class B and C devices support downlink communications. A Class C end-device operates in an always-on mode and wastes significant amounts of energy for idle listening required for the receptions of asynchronous downlinks. Class B end-devices – bidirectional end-devices with scheduled receive slots – support synchronous server-initiated downlinks. Class B end-devices must be time synchronized with the gateway which transmits beacons at every beacon period of 128 seconds. Once being synchronized, Class B end-devices wake up at each beacon period to maintain the synchronization. LoRa discretizes the time into so-called ping slots each of which is 30 msec long. One beacon period contains 4096 ping slots, and a device can request 2^k ($0 \leq k \leq 7$) ping slots per beacon period. The first ping slot position is determined randomly, and p -th ping slot starts at $t_{BEACON_RESERVED} + (r_0 + (p - 1) \times 2^{12-k}) \times 30$ where $t_{BEACON_RESERVED}$ is the time when the *BEACON_RESERVED* finishes; r_0 is the first offset randomly selected. Figure 3.3 shows the

beacon timing and an example of Class B end-devices' ping slot schedules (nodes X and Y) whose parameters are $k = 3$ and $r_0 = 4$, and $k = 4$ and $r_0 = 7$, respectively.

The downlink protocol for Class B end-devices incurs significant overheads. In addition to beacons, they must blindly wake up at their reserved ping slots regularly even though there are no buffered frames for them. Also, devices consume energy to maintain a precise clock to catch the interrupts during ping slots. We design and implement a new downlink scheme to reduce such overheads.

Chapter IV

Downlink Communications Scheme

There can be many alternative methods for downlink transmissions. One simple method is to utilize the Class A uplink-downlink transaction; an end-device periodically transmits probe messages to the server, and if there is a downlink message for the device, the server sends it as a response to the uplink probe. This method is effective and energy efficient if end-devices can guess the existence of downlink messages correctly. However, exact prediction of downlinks is practically impossible. Because end-devices cannot predict when downlink packets are ready, they can issue either too many unnecessary probes when the probing interval is short or suffer from long latencies when the probing interval is long.

Broadcasting is an effective mechanism to disseminate control information in a network that supports one to many communications. Indeed, IEEE 802.11 WLANs [26]—where an AP and multiple stations form a one to many network—adopt the periodic broadcast scheme to alert backlogged mobile stations in the Power Saving Mode (PSM). A WLAN AP periodically (usually every 100 msec) broadcasts a beacon message that contains Traffic Indication Map (TIM). A TIM enumerates mobile stations that have buffered downlink packets. Stations in the sleep mode wake up periodically at every beacon interval to listen TIMs. Backlogged stations then send PS-Poll frames requesting downlink packet transmissions. As soon as a station

receives a buffered frame, it falls back to the sleep mode until the next beacon. Stations without buffered downlink frames immediately return to the sleep state to minimize energy consumption.

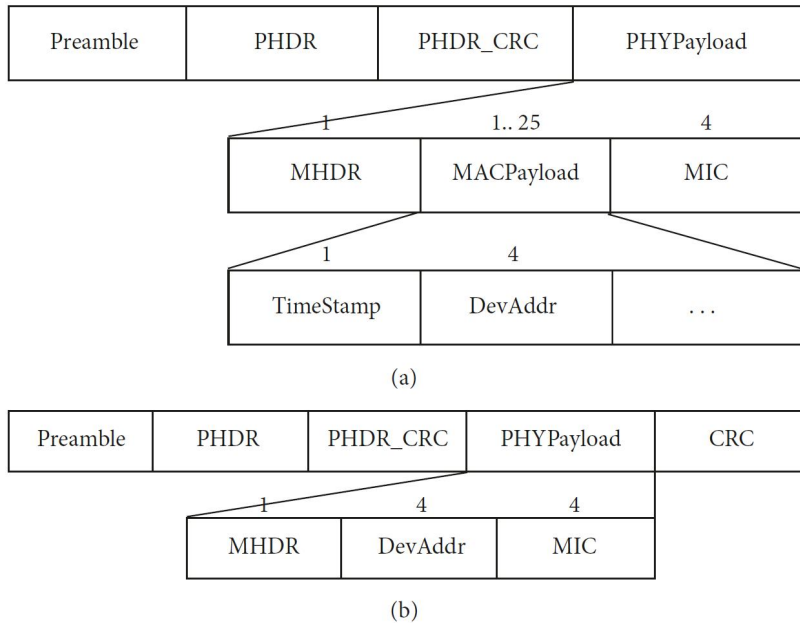


Figure 4.1: Beacon and poll message formats. (a) Beacon. (b) Poll.

Because a LoRaWAN forms a star (more precisely, a star-of-stars topology) and supports broadcasting like IEEE 802.11 WLAN, it is natural to adopt a downlink mechanism similar to the IEEE 802.11 PSM. In addition, as explained in the previous section on LoRaWAN primer, the LoRaWAN standard already supports a beacon mechanism for time synchronization. We can easily modify the structure of a LoRaWAN's beacon frame to augment a field that specifies backlogged end-devices. This additional field is similar to the TIM field of the WLAN. The message formats of beacon and poll frames are shown in

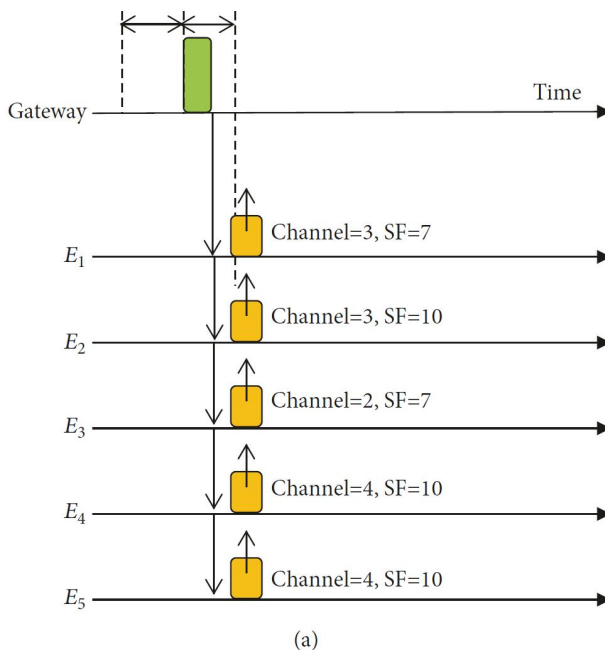
Figure 4.1. Compared to beacon transmission, polling mechanisms for LoRaWAN ask for a careful design because the MAC protocols in LoRaWAN are practically limited to the unslotted Aloha scheme. Given that carrier sensing is prohibited, a beacon triggers synchronized medium access from backlogged end-devices and causes excessive collisions. On the other hand, a LoRaWAN is robust against collisions because it supports multiple simultaneous receptions of different SFs and different subbands. In short, because polling can affect the performance of overall systems significantly, it is worthwhile to carefully analyse all aspects that may affect the performance.

4.1 Comparison of Two Polling Schemes

We consider two polling mechanisms: concurrent polling and sequential polling. Before delving into the details of polling schemes, let us first introduce the notations used for the following analysis (Table 4.1).

Table 4.1: Notations for analysis of poll mechanisms

Notation	Meaning
D_b	Size of a beacon except preamble, the minimum size is $17+4 \times m$ bytes where m is the number of end-devices with buffered downlinks
D_p	Size of a poll frame except preamble, The minimum size can be 4
D_d	Average size of a downlink frame except preamble
t_c	Time to compensate clock drift. According to the LoRaWAN standard, it is set to 13 msec
t_g	Time gap between two consecutive frames during downlink operation. Frames include poll and data
r_b	Beacon broadcasting data rate. The standard specifies to use SF=12 and the data rate is 250 bps
r_p	Average poll frame transmission data rate
r_d	Average downlink frame transmission data rate



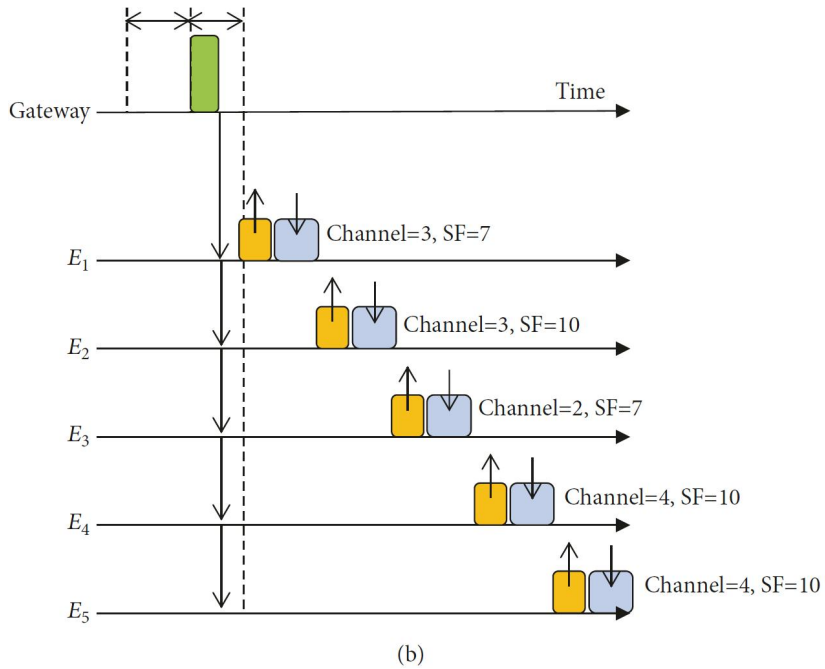


Figure 4.2: Example of polling mechanisms.
 (a) Concurrent polling. (b) Sequential polling.

Concurrent polling is designed to best exploit the characteristics of the LoRa's PHY layer. Note that a gateway can receive multiple signals simultaneously if their channels or SFs are different. Commercially available gateways support concurrent demodulation up to 8 signals; however, let us assume that the number of simultaneous receptions is increased multiplicatively by deploying multiple gateways. For example, if a LoRa network uses 10 channels and 6 different SFs as in Europe, then the maximum of 60 polls can be delivered simultaneously when more than or equal to 8 gateways are deployed. Let busy and idle devices be end-devices with and without pending downlink frames, respectively. Hearing a beacon, all busy end-devices transmit polls to the server simultaneously as shown in Figure 4.2(a).

Polls that are in the same subchannel and of the same SF will experience collisions and will be lost. For example, polls from devices E_1, E_2 , and E_3 are transmitted successfully. However, polls from devices E_4 , and E_5 will collide and will be lost.

Let n and m be the number of the maximum simultaneous frames that the network allows and the number of frames that arrive during a beacon period (i.e., the number of polls assuming that there is at most one frame per end-device). The expected number of successful polls is $m \times e^{-m/n}$, approximately. Because collided polls will compete again at the next beacon interval, the actual number of polls competing at each beacon is approximated as $m' = m + m(1 - e^{-m/n})$.

Idle devices fall back to the sleep state as soon as they recognize there are no frames for them. The maximum wake-up time of an idle device during a beacon period, W_I^C , is computed as follows.

$$W_I^C = t_c + \frac{D_b}{r_b} \quad (1)$$

A busy end-device transmits a poll and waits until it receives its downlink. As soon as it receives the downlink, it turns its radio off until the next beacon. Because the gateway transmits downlinks only to the end-devices whose polls are successfully received, on the average, $m' \times e^{-m'/n}$ downlink frames will be transmitted. The average maximum wake-up time of a busy device whose poll is delivered successfully to the gateway is

$$W_{BS}^C = t_c + \frac{D_b}{r_b} + \frac{D_p}{r_p} + \frac{1}{2} \times \left(t_g + \frac{D_d}{r_d} \right) \times m' \times e^{-m'/n} \quad (2)$$

A busy device whose poll fails to reach to the gateway must wait until all downlink transmissions are completed, and its wake-up time

is

$$W_{BF}^C = t_c + \frac{D_b}{r_b} + \frac{D_p}{r_p} + (t_g + \frac{D_d}{r_d}) \times m' \times e^{-m'/n} \quad (3)$$

Under a simple assumption that all end-devices are equally probable to have a pending downlink frame, the sum of wake-up times of all M devices under the synchronous polling scheme is

$$(M - m') \times W_I^C + m' \times e^{-m'/n} \times W_{BS}^C + m' \times (1 - e^{-m'/n}) \times W_{BF}^C \quad (4)$$

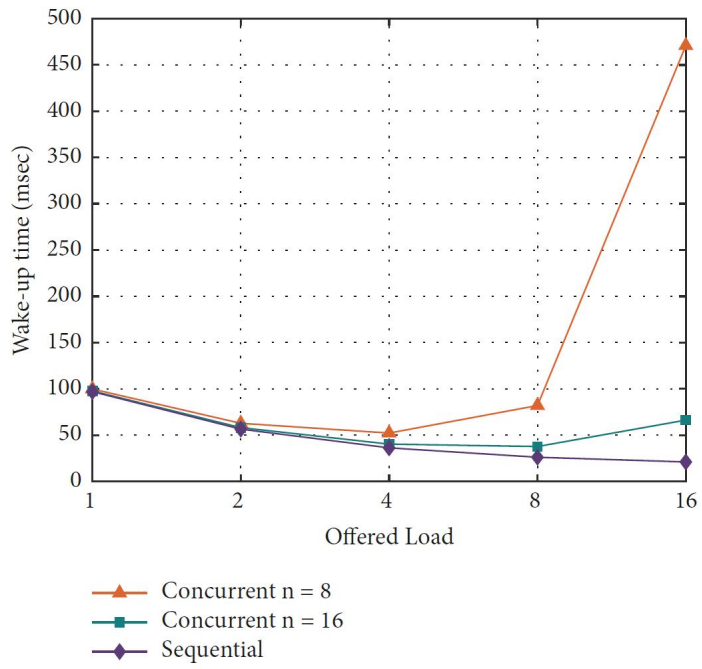
The average time that a node should turn on its battery to receive a downlink is derived by dividing (4) by the multiplication of M and the average number of successful downlinks per beacon period.

Another scheme that we have considered is sequential polling. Unlike the contention based concurrent polling, end-devices poll and receive downlink in the same order in which their addresses appeared in the DevAddr fields of a beacon frame. Figure 4.2(b) shows an example of sequential polling. Receiving a beacon, busy devices remember their positions in the DevAddr field and all devices except the first busy device fall back to the sleep state. The first busy device transmits a poll and receives a downlink frame. The second busy device wakes up after one poll-data frame exchange time to poll and receive its downlink. The same procedure repeats for succeeding busy devices. Equation (5) is the average maximum wake-up time of a busy device.

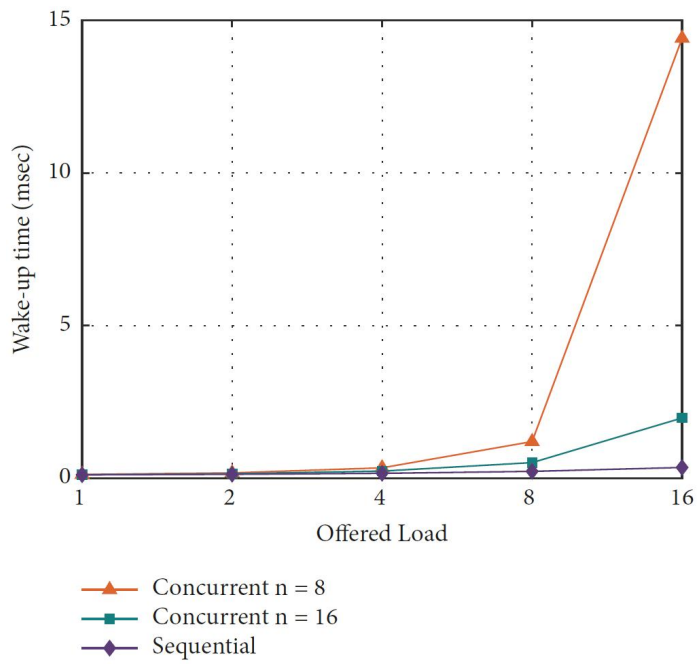
$$W_B^S = t_c + \frac{D_b}{r_b} + \frac{D_p}{r_p} + (t_g + \frac{D_d}{r_d}) \quad (5)$$

Moreover, the sum of all wake-up times during a beacon period is

$$(M - m) \times W_I^S + m \times W_B^S \quad (6)$$



(a)



(b)

Figure 4.3: Performance of concurrent polling and sequential polling.

- (a) Average wake-up time of both idle and busy devices.
- (b) Average wake-up time of busy devices.

We compared the two polling methods by varying the values of parameters that may affect performance. The performance metric is the average wake-up time required for the reception of one downlink frame. We varied the total number of end-devices (M) in a network, the number of downlink messages per beacon interval, and the network capacity for concurrent transmissions (n). Figure 4.3 shows the average wake-up times of concurrent and sequential polling as functions of the offered load. The unit of the offered load is the number of new downlink frames generated per beacon interval. Figures 4.3(a) and 4.3(b) are the wake-up time of all end-devices including both idle and busy devices and the wake-up time of busy devices only, respectively. When calculating the wake up time of busy devices only, terms $(M-m') \times W_I^C$ and $(M-m) \times W_I^S$ in equation (4) and (6) are excluded. We used two values ($n=8$ and $n=16$) of network capacity to analyse the effect of maximum simultaneous receptions. For simplicity, we assume that reception paths of gateways are ideally utilized as each gateway does not lock on the same packet. In both Figures 4.3(a) and 4.3(b), we can observe that sequential polling is more effective in power conserving than concurrent polling. When the offered load is small, the performance differences are not great; however, as the offered load increases, the gap increases also and at $m=16$, concurrent polling consumes 3 to 22 times more energy than sequential polling in the case of all devices (Figure 4.3(a)). Moreover, in the case of busy devices only (Figure 4.3(b)), concurrent polling consumes 5.5 to 41 times more energy than sequential polling. The

number of total end-devices is fixed at 1000. We performed the same analysis by varying the value of M and obtained the similar results.

We also can observe that concurrent polling at $n=16$ is better than that at $n=8$. As n increases, the probability of collision decreases. Collisions affect the performance in two ways. A device, whose poll fails to reach a gateway, wastes energy because it should wait until all downlinks are completed. Also, collisions increase the offered load at the following beacon period, and an inflated load again increases the collision probability. Generally, the wake-up time of all devices decreases as the offered load increases up to 4 (Figure 4.3(a)). However, as the offered load exceeds network capacity (n), wake-up time increases sharply.

4.2 Proposed Downlink Communications Scheme

Because our analytic study reveals the performance advantage of sequential polling over concurrent polling, we adopt sequential polling for our downlink communication scheme. Figure 4.4 illustrates TRILO in a greater detail. Beacon Window is divided into downlink reception time and uplink transmission time. After a beacon, busy devices receive downlink frames sequentially during downlink time. After that, nodes transmit uplink messages like plain Class A devices. One problem is that uplink transmissions or the downlinks responding to uplinks may overlap with the following beacon. To avoid the problem, the Beacon Guard is introduced; end-devices refrain from initiating new uplink transmissions if remaining time to the next beacon is less than Beacon Guard. Note that LoRaWAN standard limits maximum

payload size, so that beacon payload cannot convey a large number of DevAddrs; however, it can be easily extended depending on network conditions by using low SFs for beacons or allocating short network addresses to end-devices.

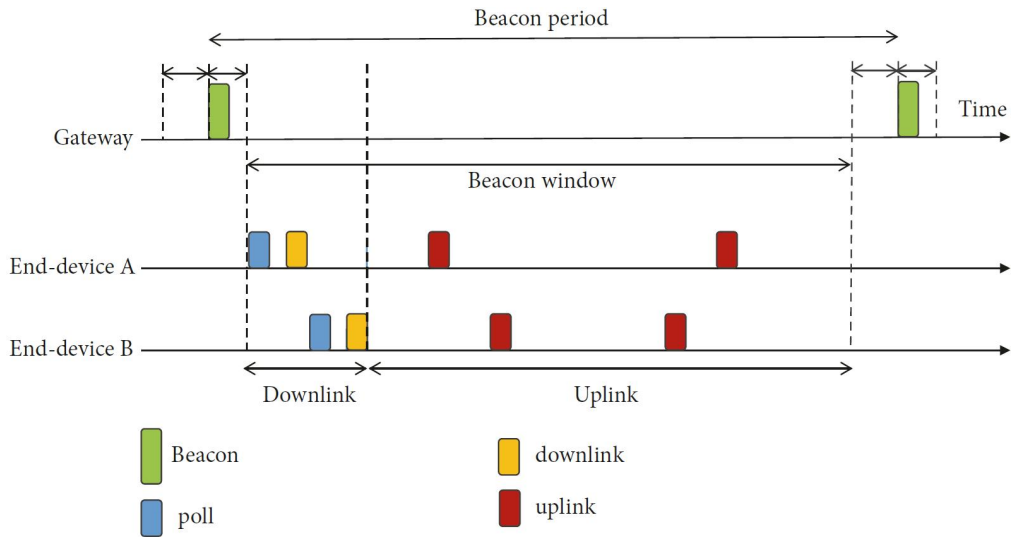


Figure 4.4: Proposed downlink communication scheme.

Chapter V

Implementation



Figure 5.1: Devices used for implementation. (a) End-device with SX1272MB2DAS attached to a NUCLEO-L073RZ board. (b) Gateway with RAK831 attached to a Raspberry Pi 3.

We implemented TRILO using commercially available components. We built a gateway on a RAK831 board [27] which contains an SX1301 concentrator chip. The gateway board is attached to a Raspberry Pi 3 board as shown in Figure 5.1(b). For our implementation, we employed the Semtech libraries which contain LoRaWAN packet forwarder and hardware abstraction layer for SX1301.

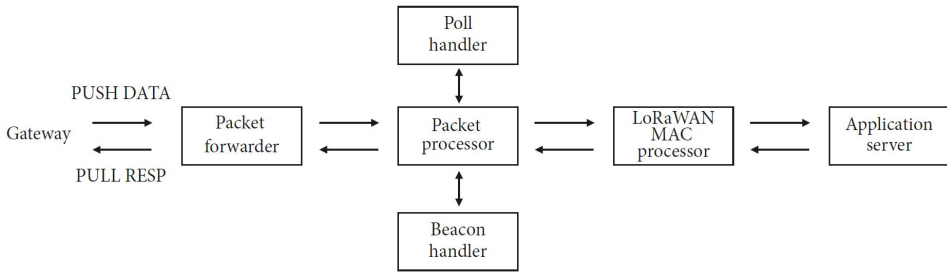


Figure 5.2: Block diagram of a network server that handles beacon and poll messages.

In the LoRaWAN architecture, a gateway plays a simple role of a bridge between end-devices and a network server, and a network server performs all beacon and poll message processings. We utilize an open source project [28], targeted for private LoRaWAN network production in implementing a network server. Figure 5.2 describes the message handler modules that we implemented. The beacon handler creates a beacon payload consisting of the timestamp and buffered downlink frame information. Then it passes the payload to the packet processor which assembles the payload into a beacon packet. Since a beacon needs to be transmitted in a greater time precision than data packets, we modified the gateway such that beacons are transmitted immediately. The poll handler sends a pending downlink frame in response to a poll message. Note that this mechanism is transparent to the LoRaWAN MAC processor and the application server because we implemented modules at the packet processor level.

An end-device is implemented on a NUCLEO-L073RZ board with an embedded LoRaWAN chip using a 915Mhz antenna (see Figure 5.1(a)). We attached the SX1272MB2DAS component to a NUCLEO-L073RZ board with the modified LoRa MAC. Note that end-device logics are

compiled and stored as firmware in an end-device. Time synchronization between nodes and a network server is based on the local time of a network server instead of GPS time because we implemented the beacon handler at the server, not using the beacon frame of the Class B standard. We modified the end-device's software by adding the beacon handling and polling functions. Note that each device which has a pending frame waits for its turn, and processing times of each downlink vary due to different SFs. In a downlink period, we configured the time for each poll and downlink based on SF 12 which has the longest airtime. However, the experimental results show that the proposed scheme can be deployed with high performance even with the conservative configuration. It is possible to optimize the waiting times for each downlink more compactly based on the information about SFs of each node; however, we leave this issue as future work.

We tuned radios of the components to obey the Korean regulation which allocates frequency bands from 920Mhz to 923Mhz for LoRaWAN. We also added the listen before talk (LBT) function as the regulation specifies. Note that the current LoRaWAN specifications for the KR920-923 ISM band do not have duty cycle limits but require adopting the LBT channel access rule [4].

Chapter VI

Evaluation

We evaluate the performance of TRILO by deploying modified components in our office building. We placed the gateway and three end-devices in our lab. Also, we deploy 12 more end-devices on the same floor of the building as shown in Figure 6.1. The beacon periods are set to either 128 sec. or 256 sec. We varied the uplink and downlink offered loads from 1, 2, 4 to 8 frames per beacon period. The offered traffic is unrealistically large for such a small network; however, note that we are trying to emulate the operating conditions of large scale LoRaWAN networks consisting of tens of thousands of end-devices. Testbeds of such scale are not available, so our experiment emulates large networks with 15 end-devices. Thus, Uplink and downlink messages should be interpreted as an aggregated traffic generated by thousands of end-devices. Message interarrival times of uplink and downlink traffic follow the exponential distribution, and the destinations of downlink messages are randomly and uniformly selected. We used primitive Adaptive Data Rate (ADR) for SF and power allocation, and all nodes converged to SF 8 and default EIRP output power (14dBm). The performance of real-world LoRaWAN networks depends on the distributions of SF and transmission power; however, we ignore these factors because improvement of uplink transmissions is not a goal of this work.

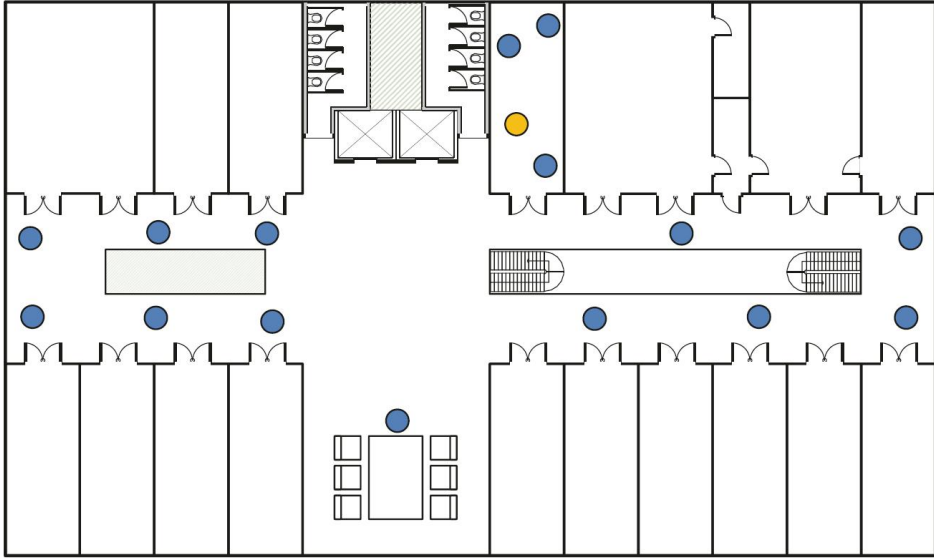


Figure 6.1: Experiment environment. One gateway (yellow dot) and 15 end-devices (blue dots) are deployed in our office building.

The performance metrics used in this study include Packet Delivery Ratio (PDR), duty cycle, and latency. To obtain reliable results, we repeat experiments with the same parameter values ten times. The length of each experiment run is 10 beacon periods (i.e., 1,280 or 2,560 sec). Because the destinations of downlinks and the origins of uplinks are randomly selected, it is expected that all end-devices and messages experience the average performance.

6.1 Experimental Results

First of all, we measure the PDR of uplink and downlink frames. We observe that all downlink frames are delivered successfully without

exception. The result is rather surprising because TRILO employs beacon broadcasting and polling in addition to downlink data frames. A failure in any one component may lead to unsuccessful data transmissions. Unlike downlink frames, uplink traffic experiences occasional transmission failures. We measure the PDR by varying the offered loads of both uplink and downlink traffic. Note that all nodes use the same SF, and collisions occur if frames are transmitted on the same channel simultaneously. Table 6.1 illustrates the PDR of uplink traffic at different offered loads. Both uplink and downlink traffic affect the PDR of uplink traffic. The PDR decreases as the offered load of downlink traffic increases; at $\lambda_u = 2$, the PDR decreases from 98.64% to 97.72% as the offered load of downlink traffic increases from 1 to 4. In addition, the uplink traffic intensity also affects the PDR of uplink traffic; for example, at $\lambda_d = 2$, the PDR decreases from 98.27% to 96.03% as the offered load of uplink traffic increases from 2 to 8.

Table 6.1: Packet delivery ratio of uplink traffic at various uplink and downlink offered loads.

Packet generation rate	$\lambda_d = 1$	$\lambda_d = 2$	$\lambda_d = 4$
$\lambda_u = 2$	98.64%	98.27%	97.72%
$\lambda_u = 8$	96.74%	96.03%	95.10%

Note that uplink transmissions are prohibited during polling and following downlink frame transmissions. Uplink frames which arrive during downlink operation should wait until the current downlink operation is completed. This waiting procedure synchronizes backlogged end-devices and may cause collisions. Even though the LoRa PHY supports multiple simultaneous transmissions of different SFs or channels, multiple attempts increase the collision probabilities

and the PDR decreases as both uplink and downlink traffic increase. To reduce the bloated collisions due to synchronous transmissions, persistent mechanisms such as 0-persistence or p-persistence are required. However, persistence schemes increase the complexity of the network protocol and may cause other side effects such as increased energy consumption.

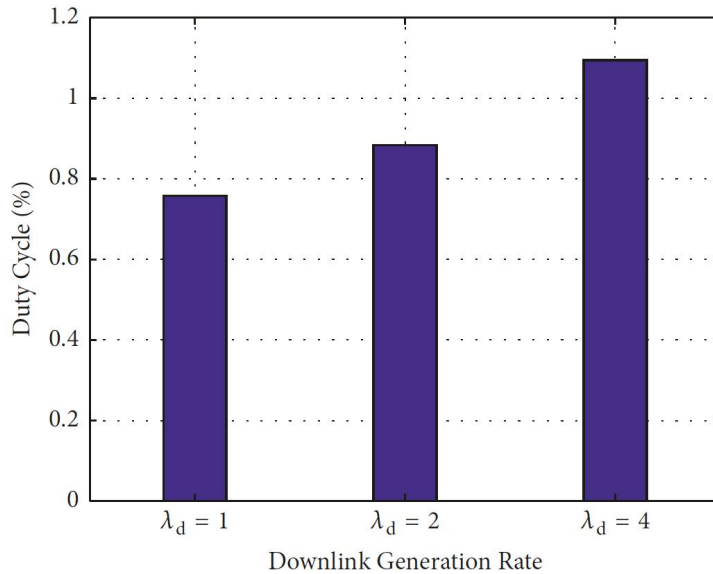
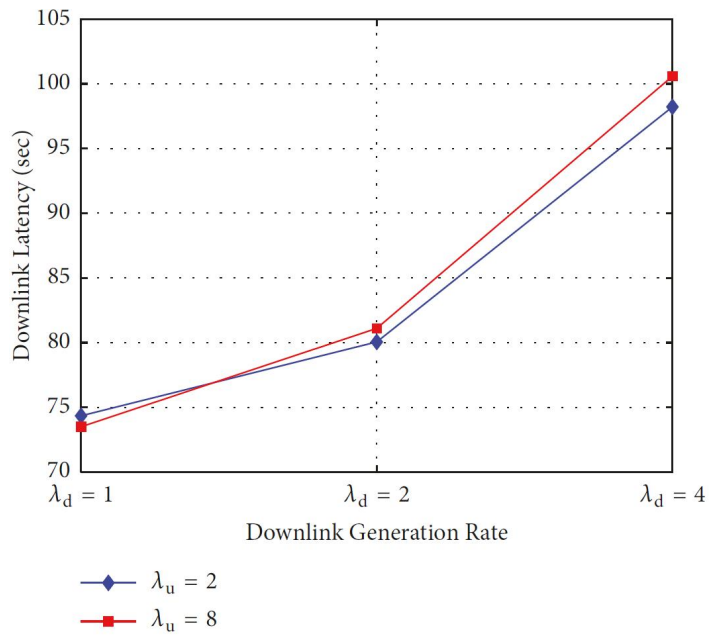


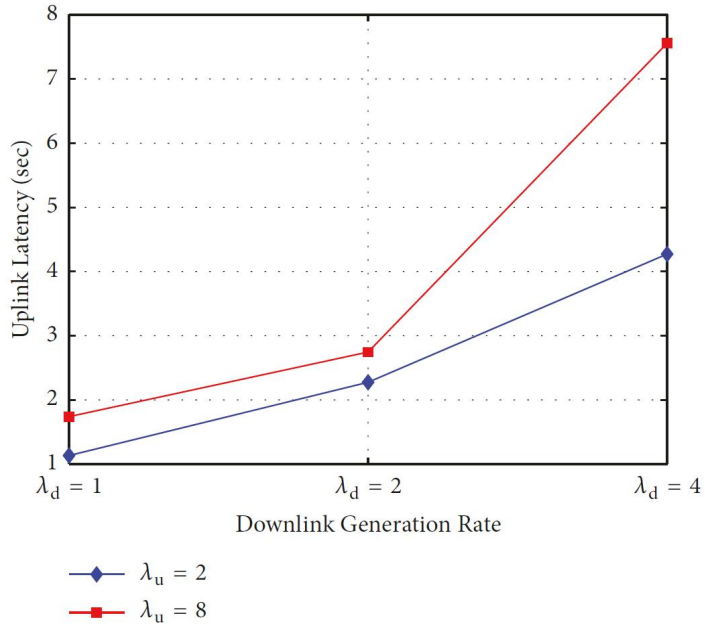
Figure 6.2: Duty cycles required for downlink operation including beacon, poll, and downlink data transmissions.

Next, we assess the additional power consumed for downlink communications. Because gateways operate in an always-on mode, we only measure the energy consumed by end-devices. We use the duty cycle, additional time required for downlink communications, as the performance metric. The duty cycle is the sum of wake-up times used for beacon reception, for possible poll transmission, and for downlink data frame receptions. Figure 6.2 shows the average duty cycle at

different downlink traffic loads. The duty cycle increases as the downlink offered load increases; it increases from 0.75% to 1.1% as λ_d increases from 1 to 4. Note that all end-devices consume the minimal fixed duty cycle for beacon reception regardless of the intensity of downlink traffic. In addition to the fixed duty cycle for beacon reception, end-devices with backlogged downlinks continue to stay in the wake-up state for polling and data reception.



(a)



(b)

Figure 6.3: Average latency of traffic.

(a) Downlink latency. (b) Uplink latency.

Figure 6.3 illustrates the average latency of downlink traffic and uplink traffic as functions of offered load, respectively. As shown in Figure 6.3(a), the average latency of downlink traffic increases in proportion to the offered load. As explained before, downlink frames are generated according to a Poisson process. Therefore, the probability that a downlink frame occurs in a small time period follows uniform distribution and, on average, each downlink frame waits one-half of the beacon interval. In addition, frames that arrive during a downlink processing are postponed to the next beacon. In Figure 6.3(a), we can observe that the effect of uplink traffic on the average latency of downlink is minimal. This result is not surprising because uplink and downlink communications are well isolated in the proposed

scheme.

Like the average downlink latency, the average uplink latency increases as the downlink offered load increases. Uplink frames that arrive during downlink periods should wait until the end of the current downlink period. The average latency of uplink traffic as well as the duty cycle increase as the downlink offered load increases. Contrary to Figure 6.3(a) where the average downlink latency is seldom affected by the uplink offered load, the average uplink latency increases proportionally as the uplink offered load increases. As the uplink communication demands increase, a queue starts to form, and this causes the increase in waiting time. The queueing time is most distinctive at $\lambda_d = 4$ when the service time for uplink communications is minimal.

6.2 Simulation Results

We also compared the performance of the Class B downlink scheme and that of TRILO. Because commercial LoRaWAN devices do not support Class B functions yet, we relied on computer simulations for the performance comparison. The simulation code is written primarily in C/C++, and we conduct extensive simulations in a typical LoRaWAN network and in a heavy downlink traffic condition, respectively. To compare energy consumed for downlink communications, we define the efficiency of each protocol as a performance metric. The efficiency, defined as the ratio of data transmission time to the duty cycle, is the fraction of time used for

useful work.

According to the LoRaWAN standard, implementation of the Class B downlink scheme discretizes the time into so-called ping slots. Each end-device requests 2^k ($0 \leq k \leq 7$) ping slots per beacon period. We use the average case of the Class B where each end-device randomly selects a value of the parameter k between 0 and 7. Let us first introduce the notations for the analysis of LoRaWAN downlink protocol (Table 6.2).

Table 6.2: Notations used for Class B downlink protocol and TRILO.

Notation	Meaning
D_T	Duty cycle of TRILO
D_B	Duty cycle of the Class B downlink protocol
T_{Beacon}^T	Beacon transmission time of TRILO
T_{Beacon}^B	Beacon transmission time of the Class B downlink protocol
T_{poll}	Average poll frame transmission time
T_{slot}	Time allocated for a ping slot (30 msec)
T_{down}	Average downlink frame transmission time
k	Parameter for the Class B's ping slots
I_E	Indicator function representing a node is backlogged or not

We used SF 9 for beacon transmissions according to the LoRaWAN specification, KR 920–923 [29]. The duty cycle of TRILO, D_T , is

$$D_T = \frac{T_{Beacon}^T + I_E \times (T_{poll} + T_{down})}{BeaconPeriod} \quad (7)$$

Note that unlike T_{Beacon}^B , T_{Beacon}^T increases in proportion to the number of busy end-devices. The duty cycle of a Class B device, D_B , is

$$D_B = \frac{T_{Beacon}^B + 2^k \times T_{slot} + I_E \times (T_{down} - T_{slot})}{BeaconPeriod} \quad (8)$$

Class B devices have different duty cycles depending on randomly selected values of parameter k . Then, the efficiency is computed as

$$Efficiency = \frac{Downlink\ transmission\ time}{Duty\ cycles} \quad (9)$$

We measured the efficiency of TRILO and the Class B downlink protocol by varying the number of nodes from 50 to 4000 and the downlink offered load from 2 to 32 frames per beacon period. Each performance point is the average of 10,000 runs. We limit the maximum downlink traffic to 32 frames per beacon interval because uplink traffic is greater than downlink traffic in many LoRaWAN applications. Note that at $\lambda_d = 32$, about a half of beacon period is consumed for downlink communications if we assume that the downlink transmission time is 2 seconds on average.

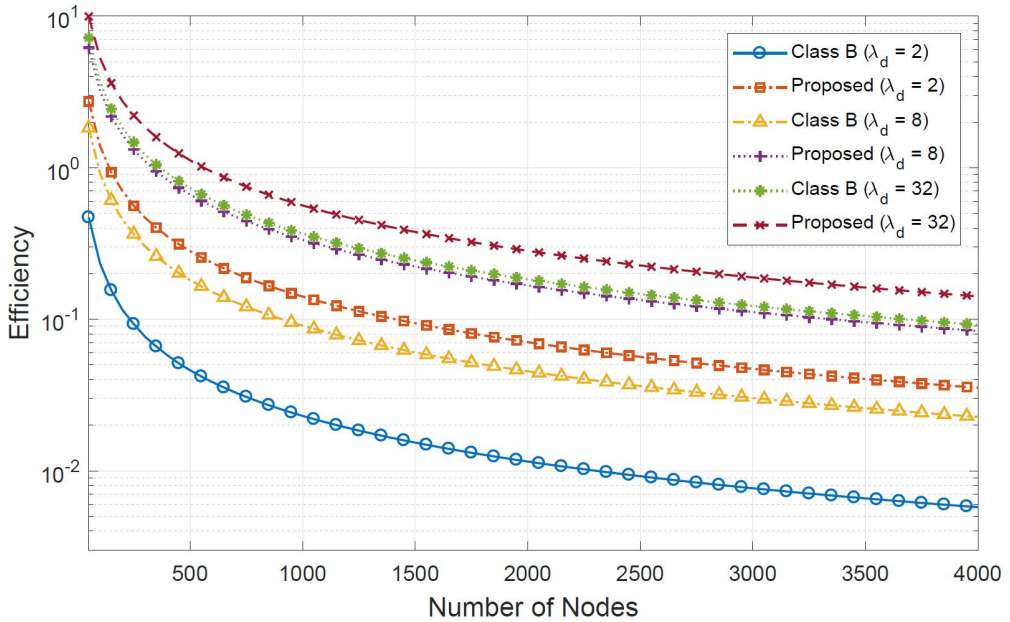


Figure 6.4: Efficiency of TRILO and Class B downlink protocol.

The efficiency of each scheme is shown in Figure 6.4. Note that the offered load is aggregated load and the traffic intensity of individual node decreases as the number of nodes increases. The total times for downlink communications are fixed at each given offered load. However, the sum of duty cycles increases as the number of nodes increases. Therefore, in both protocols, the maximum efficiencies are realized at small networks, and the efficiency decreases as the network size increases. The results illustrate that efficiencies of TRILO are higher than those of the Class B downlink protocol throughout all downlink generation rates. The Class B scheme performs well in heavy traffic cases. However, the proposed scheme outperforms the Class B scheme even in heavy traffic conditions. In small networks, the performance gap decreases from about 5.8 times to about 1.4 times as λ_d increases from 2 to 32. Also, each gap in each offered load

increases as the network size increases (from about 6.1 times to about 1.5 times). In the case of TRILO, the average duty cycle decreases inversely proportional to the number of nodes because only busy devices are active during downlink periods. On the contrary, Class B protocol allocates about 31 ping slots on average regardless of downlink demands. In short, the number of receive windows wasted by the Class B scheme varies depending on the amount of downlink traffic. However, only busy devices use extra duty cycle for downlink traffic in TRILO.

The Class B protocol does not coordinate traffic between uplinks and downlinks, so that several uplinks can be disrupted by downlink transmissions due to the half-duplex characteristic of a LoRaWAN gateway; all reception paths can be blocked by downlink transmissions. It can obstruct the proper operations of typical LoRaWANs where uplink transmissions are predominant. In contrast, the proposed scheme is free from this problem because it isolates the time for uplinks and downlinks periods.

Chapter VII

Discussion

We would like to discuss the traffic indication mechanism that could be improved in the proposed scheme. In the proposed beacon structure, the TIM is constructed by simply adding the addresses of the nodes; However, this causes overhead in which the size of the beacon increases as the number of nodes in the network increases. Therefore, we propose a TIM construction method using bloom filter for scalability of polling based system. The bloom filter is a probabilistic data structure proposed to solve the approximate set membership problem, and information about which elements are included in a particular set can be known as $O(k)$ complexity according to the number of hash functions k . Also, when the number of items input to the bloom filter is n and the total number of bits is m , it is incorrectly determined that an item is included in the set even though it is not included in the set according to the false positive probability corresponding to the specific n , m , k values. Therefore, it is important to design a system that meets the criteria by setting the appropriate false positive probability.

We propose a 2-phase bloom filter to transmit traffic indication and sequence information using a small memory space. In a 2-phase bloom filter, the false positive probability is expressed as the product of the false positive probabilities of 1-phase and 2-phase bloom filter, thus a more robust system can be implemented. In the 1-phase bloom filter,

hashing is performed based on the address of the backlogged node. Next, In the 2-phase bloom filter, the sequence combined with the address of the backlogged node and the poll transmission order information of the node is hashed. Performances on the size of the bit array of each phase filter, $m1$, $m2$, are compared by increasing bit array size from 8 to 96. Also, the number of hash functions is set to the value that the false positive probability is minimized.

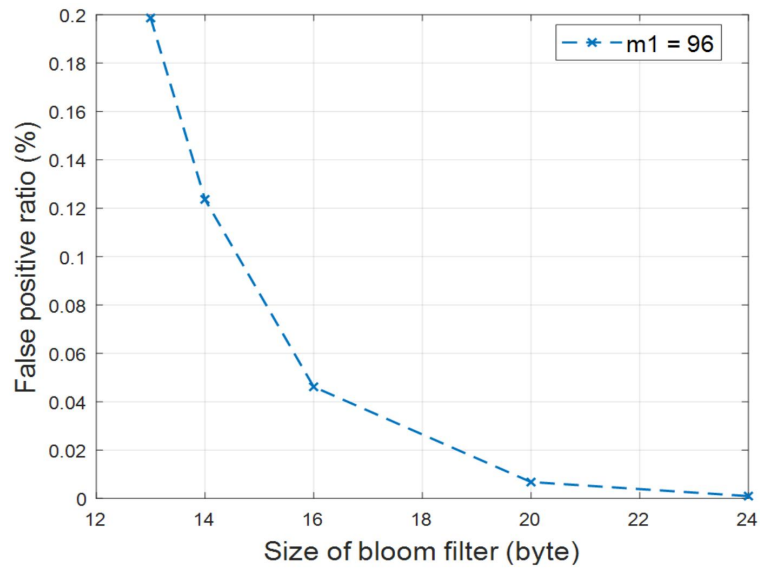


Figure 7.1 False positive ratio of 2-phase bloom filter of 96-bit array 1-phase filter with various size of 2-phase filter.

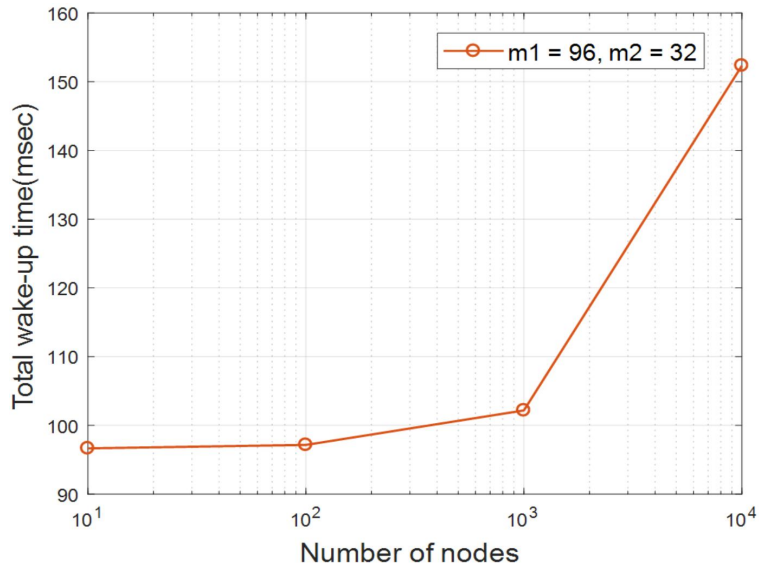


Figure 7.2 Total wake-up time for polling and downlink operation.

Figure 7.1 shows a false positive ratio that changes as the bit array size of 2-phase bloom filter is increased from 8 to 96 when the bit array size of 1-phase bloom filter is fixed at 96. We can see that the probability decreases sharply as the size of the 2-phase filter increases. We select total filter size to 16 bytes with about 0.04% false positive probability. In addition, when the bit array size of the 1-phase filter is 96 bits, the 2-phase filter is checked with a probability of only about 0.3% after the first stage to determine whether they are really backlogged or not even if 1-phase filter fails to distinguish false positive nodes. Total wake-up time for polling and downlink operation when the number of nodes increases is shown at Figure 7.2. The 2-phase bloom filter shows quite low wake-up time regardless of the number of nodes. It keeps performance similar to the address-added TIM but reduces overhead of TIM size with more scalability.

Chapter VIII

Conclusion

A plethora of LPWAN techniques such as LoRa, SigFox, RPMA, and Weightless have emerged as a new enabling network technology for IoT applications that require low-rate, low-cost, and long lifetimes. LPWANs allow end-device initiated uplinks. However, to maximize the lifetime of battery powered end-devices, nodes are put into the sleep state such that rather restricted downlink communications are permitted. In this thesis, we proposed a new downlink protocol, named TRILO, for LoRaWAN.

Because LoRaWAN assumes a star topology where multiple end-devices are connected to a single gateway, we adopted a beacon based downlink mechanism similar to the IEEE 802.11 PSM standard. A gateway broadcast beacons periodically at every beacon period and end-devices are time synchronized. Beacons alert nodes with buffered downlinks in addition to synchronizing end-devices' clocks. Customized to the physical characteristics of LoRa, we designed two polling schemes: concurrent polling and sequential polling. An analysis indicates that sequential polling is more energy efficient than concurrent polling.

We implement the proposed beacon based downlink protocol using commercially available components and conduct experiments with modified devices. Our performance study shows that Packet Delivery

Ratio (PDR) is almost 100% for both uplink and downlink traffic, and the extra wake-up time to receive beacons and downlinks is minimal. Simulation results also show that our proposed protocol can adaptively allocate receive windows resulting in lower energy consumption.

For further work, we plan to investigate the impact of our scheme on the networks with multiple gateways. Also, detailed investigations of the impact of the number of downlinks, and the certain distributions of SFs on the performance seem interesting. Optimization techniques leveraging SF and power allocation are expected to affect the performance of the proposed scheme.

BIBLIOGRAPHY

- [1] M. Bor, U. Roedig, T. Voigt, and J. M. Alonso, “Do LoRa low-power wide-area networks scale?” in Proceedings of the 19th ACM International Conference on Modeling, Analysis and Simulation of Wireless and Mobile Systems, MSWiM 2016, pp. 59 - 67, Malta, November 2016.
- [2] D.Magrin, M.Centenaro, and L.Vangelista, “Performance evaluation of LoRa networks in a smart city scenario,” in Proceedings of the 2017 IEEE International Conference on Communications, ICC 2017, France, May 2017.
- [3] LoRa, <https://www.lora-alliance.org/What-Is-LoRa/Technology>.
- [4] “LoRaWAN 1.1 specification,” LoRa Alliance, 2017, <https://lora-alliance.org/resource-hub/lorawantm-specification-v11>.
- [5] M. Bor, J. Vidler, and U. Roedig, “LoRa for the internet of things,” in Proceedings of the International Conference on mbedded wireless Systems and Networks (EWSN '16), pp. 361 - 66, Junction Publishing, 2016.
- [6] 3GPP, “Study on provision of low-cost Machine-Type Communications User Equipments based on LTE,” TR 36.888 12.0.0, 6, 2013.
- [7] 3GPP, “Cellular system support for ultra-low complexity and low throughput Internet of Things,” TR 45.820 V13.1.0, 11, 2015.
- [8] J. Gozalvez, “New 3GPP Standard for IoT,” IEEE Vehicular Technology Magazine, vol. 11, no. 1, pp. 14 - 20, 2016.

- [9] R. Ratasuk, N. Mangalvedhe, and A. Ghosh, "Overview of LTE enhancements for cellular IoT," in Proceedings of the 26th IEEE Annual International Symposium on Personal, Indoor, and Mobile Radio Communications, PIMRC 2015, pp. 2293 - 2297, China, September 2015.
- [10] H. Shariatmadari, R. Ratasuk, S. Irajii et al., "Machine-type communications: current status and future perspectives toward 5G systems," IEEE Communications Magazine, vol. 53, no. 9, pp. 10 - 17, 2015.
- [11] S. Landstrom, J. Bergstrom, E. Westerberg, and D. Hammar wall, "NB-IoT: a sustainable technology for connecting billions of devices," Ericsson Technology Review, vol. 4, pp. 2 - 11, 2016.
- [12] M. Lauridsen, I. Z. Kovacs, P. Mogensen, M. Sorensen, and S. Holst, "Coverage and capacity analysis of LTE-M and NB-IoT in a rural area," in Proceedings of the 2016 IEEE 84th Vehicular Technology Conference(VTC-Fall), pp. 1 - 5, Montreal, QC, Canada, September 2016.
- [13] Sigfox, <http://www.sigfox.com>.
- [14] Weightless open standard, <http://www.weightless.org>.
- [15] Ingenu RPMA, <http://www.ingenu.com/technology/rpma>.
- [16] A. Dunkels, "The ContikiMAC radio duty cycling protocol," Technical Report T2011:13, Swedish Institute of Computer Science, 2011.
- [17] J. Ko, J. Eriksson, N. Tsiftes et al., "Industry: Beyond interoperability - Pushing the performance of sensor network IP stacks," in Proceedings of the 9th ACM Conference on Embedded

Networked Sensor Systems, SenSys 2011, pp. 1 - 11, USA, November 2011.

- [18] D. Moss, J. Hui, and K. Klues, "TEP 105: low power listening," <http://www.tinyos.net/tinyos-2.x/doc/pdf/tep105.pdf>, 2008.
- [19] C. Gomez, J. Oller, and J. Paradells, "Overview and evaluation of bluetooth low energy: an emerging low-power wireless technology," *Sensors*, vol. 12, no. 9, pp. 11734 - 11753, 2012.
- [20] A.A. Kandhalu, A. E. Xhafa, and S. Hosur, "Towards bounded latency bluetooth low energy for in-vehicle network cable replacement," in *Proceeding of the International Conference on Connected Vehicles and Expo (ICCVE)*, pp. 635 - 640, Las Vegas, NV, USA, 2013.
- [21] A. Montanari, S. Nawaz, C. Mascolo, and K. Sailer, "A study of bluetooth low energy performance for human proximity detection in the workplace," in *Proceedings of the 2017 IEEE International Conference on Pervasive Computing and Communications, PerCom 2017*, pp. 90 - 99, Kona, HI, USA, March 2017.
- [22] C. Julien, C. Liu, A. L. Murphy, and G. P. Picco, "BLEnd: Practical continuous neighbor discovery for bluetooth low energy," in *Proceedings of the 16th ACM/IEEE International Conference on Information Processing in Sensor Networks, IPSN 2017*, pp. 105 - 116, New York, NY, USA, April 2017.
- [23] Y. Qiu, S. Li, X. Xu, and Z. Li, "Talk more listen less: energy efficient neighbor discovery in wireless sensor networks," in *Proceedings of the 35th Annual IEEE International Conference on Computer Communications, IEEE INFOCOM 2016*, USA, April 2016.
- [24] A. J. Berni and W. D. Gregg, "On the utility of chirp modulation

for digital signaling,” IEEE Transactions on Communications, vol. 21, no. 6, pp. 748 - 751, 1973.

- [25] A. Springer, W. Gugler, M. Huemer, L. Reindl, C. C.W. Ruppel, and R. Weigel, “Spread spectrum communications using chirp signals,” in Proceedings of the IEEE/AFCEA Information Systems for Enhanced Public Safety and Security, EUROCOMM 2000, pp. 166 - 170, Germany.
- [26] IEEE Std 802.11-2007, “IEEE Standard for Information Technology – Telecommunications and Information Exchange between Systems – Local and Metropolitan Area Networks – Specific Requirements Part 11: Wireless LAN Medium Access Control (MAC) and Physical Layer (PHY) Specifications, June 2007”.
- [27] RAK831, <http://www.rakwireless.com/en/WisKeyOSH/RAK831>.
- [28] LoRaWAN network server,
<https://github.com/gotthardp/lorawan-server>.
- [29] “LoRaWAN 1.1 Regional Parameters,” LoRa Alliance, 2017,
<https://lora-alliance.org/resource-hub/lorawantm-regional-parameters-v11ra>.

요 약

트래픽 알림을 활용한 폴링 기반 LoRaWAN 다운링크 통신 프로토콜

오영준

컴퓨터공학부

서울대학교 대학원

전력 공급이 제한적인 수 만개의 디바이스들을 이용하여 넓은 지역을 바탕으로 운영되는 사물인터넷 시스템을 구축하는 데에 있어서 LoRa, SigFox와 같은 저전력 광역 네트워크 기술(LPWA)이 주목받고 있다. 이러한 시스템 환경에서 에너지 절약은 중요한 관심사 중 하나이며 네트워크 프로토콜들은 다양한 절전 방식을 채택하여 디바이스의 수명을 보장하려 하고 있다. 예를 들어, 불필요한 대기 청취로 인한 에너지 손실을 방지하기 위해서 LoRaWAN은 다운링크 통신을 제한하고 있는데, 이러한 설계 철학은 비동기적인 다운링크 통신을 필요로 하는 IoT 애플리케이션의 요구 사항을 충족시키지 못하는 문제점을 가지고 있다. 따라서 본 논문에서는 LoRaWAN에서 다운링크를 효과적으로 컨트롤할 수 있도록 TRILO라는 에너지 효율적인 다운링크 통신 메커니즘을 설계하고 구현하였다. TRILO는 다운링크 프레임이 팬딩되어 있는 엔드 디바이스들의 리스트 정보를 주기적으로 네트워크에 알리는 비콘 메커니즘을 채택하였고, 서버와 디바이스들이 각각 정해진 순서에 따라 다운링크 전송 및 수신을 스케줄링하도록 하였다. 설계한 프로토콜이 제대로 동작하는지 검증하기 위해서 기존 LoRaWAN의 구성 요소 위에 제안된 프로토콜을 구현한 후 실제

테스트 베드를 구축하여서 실험을 진행하였다. 실험 결과에 따르면 TRILO는 기존 프로토콜의 업링크 통신 성능을 저해하지 않으면서도 추가적인 다운링크 프레임 손실 없이 성공적으로 전송 및 수신하였고, 컴퓨터 시뮬레이션 결과 또한 제안된 기법이 기존의 LoRaWAN 다운링크 프로토콜보다 더 에너지 효율적으로 동작하는 것을 보여주었다.

주요어: 저전력 광역 네트워크, 로라, 네트워크 통신 프로토콜, 다운링크 통신, 사물인터넷, 트래픽 알림

학번: 2017-26321